

Towards Batteryless Cardiac Implantable Electronic Devices – The Swiss Way

Adrian Zurbuchen, Andreas Haeblerlin, Alois Pfenniger, Lukas Bereuter, Jakob Schaerer, Frank Jutzi, Christoph Huber, Juerg Fuhrer and Rolf Vogel

Abstract—Energy harvesting devices are widely discussed as an alternative power source for today's active implantable medical devices. Repeated battery replacement procedures can be avoided by extending the implants life span, which is the goal of energy harvesting concepts. This reduces the risk of complications for the patient and may even reduce device size. The continuous and powerful contractions of a human heart ideally qualify as a battery substitute. In particular, devices in close proximity to the heart such as pacemakers, defibrillators or bio signal (ECG) recorders would benefit from this alternative energy source. The clockwork of an automatic wristwatch was used to transform the heart's kinetic energy into electrical energy. In order to qualify as a continuous energy supply for the consuming device, the mechanism needs to demonstrate its harvesting capability under various conditions. Several in-vivo recorded heart motions were used as input of a mathematical model to optimize the clockwork's original conversion efficiency with respect to myocardial contractions. The resulting design was implemented and tested during in-vitro and in-vivo experiments, which demonstrated the superior sensitivity of the new design for all tested heart motions.

Index Terms—cardiology, energy harvesting, implantable biomedical devices, optimization, pacemakers.

I. INTRODUCTION

TODAY'S active implantable medical devices play an important role in monitoring, diagnosing and treating patients. Device manufacturers invent smart and autonomous implants that improve the patient's health without imposing new device related restrictions on the patient's quality of life. However, many implants run on internal primary batteries which suffer from a limited energy storage capacity. Therefore, patients are forced to undergo repeated surgical interventions to replace their implant prior to a complete battery depletion. Furthermore, while electronic circuits steadily decrease in size, efforts to improve the batteries energy density show only little progress [1], [2]. Therefore, the battery's weight, size

The research was supported by the Commission for Technology and Innovation (KTI-CTI 12589.1 PFLS-LS), the Research Funds of the Department of Cardiology at the Bürgerspital Solothurn, Switzerland and the Department of Cardiology at the Bern University Hospital, Switzerland.

A. Zurbuchen, A. Haeblerlin, L. Bereuter and J. Schaerer are with ARTORG Cardiovascular Engineering, University of Bern, 3008 Bern, Switzerland and the Department of Cardiology, Bern University Hospital and University of Bern, 3010 Bern, Switzerland.

A. Pfenniger was with ARTORG Cardiovascular Engineering, University of Bern, 3008 Bern, Switzerland and is now with Biolab Technology AG, 8008 Zurich, Switzerland.

F. Jutzi is with Atelier für Uhren, Frank Jutzi, 3114 Wichtrach, Switzerland.

Ch. Huber is with the Department of Cardiovascular Surgery, Bern University Hospital and University of Bern, 3010 Bern, Switzerland.

R. Vogel is with the Department of Cardiology, Bürgerspital Solothurn, 4500 Solothurn, Switzerland.

and limited capacity and lifetime will remain major issues for active medical implants.

The demand for an alternative to batteries resulted in a quest for intracorporeal energy sources. Researchers are exploring strategies to harvest energy from various potential sources in the human body [3], [4]. Investigations show the possibility to harvest energy from joint motions by piezoelectric ceramics [5]–[7], chemical reactions of glucose and oxygen in dedicated fuel cells [8], sunlight penetrating the human skin by solar cells [9]–[11], body movements by using nanowire technology [12] or waste heat from the body by using thermoelectric generators [13].

The heart is another energy source which deserves special attention due to its unique properties: the myocardium is the most enduring muscle in the human body. At an average heart rate of about 70 beats per minute the heart performs more than 2.5 billion heart cycles during a human's life of 70 years. Its continuous and repetitive ventricular contractions reach high accelerations of over $2 \text{ m} \cdot \text{s}^{-2}$ [14] regardless of a person's activity. Furthermore, the heart expends a large amount of energy to maintain a constant perfusion of the human organs. The hydraulic power to maintain a cardiac output $CO = 6.3 \text{ l} \cdot \text{min}^{-1}$ at a mean aortic pressure $p_{mean} = 100 \text{ mm} \cdot \text{Hg}$ is about 1.4 W [15]. During the past few years, different groups explored ways to take advantage of this energy source such as from blood flow by an intravascular turbine [16], [17], from blood pressure gradients using a micro barrel [18] or a dual-chamber system [19] or from the ventricular wall motion by utilising piezoelectric ceramics [20]–[23] or electromagnetic systems that base on oscillatory rotational generators similar to the method presented in this study [4], [24], [25]. All these energy harvesting systems are located in close proximity to the heart and are therefore well suited for powering cardiac pacemakers. In addition, pacemakers would benefit from these alternative energy sources in two ways: First, pacemaker leads which may cause complications (e.g. lead dislocation, fracture or infection [26]) and pose an imminent threat to patients are not needed anymore. Second, by avoiding batteries, patients could be spared from surgical re-interventions. Currently, approximately 25% of all pacemaker replacements are related to depleting batteries [27]. Especially for young patients this is a crucial factor [28].

In this study we investigate the clockwork mechanism of an automatic wristwatch that has been utilized to transform heartbeat motion into electrical energy. Automatic clockworks were invented in the year 1769 and they are known to be reliable, precise and long lasting mechanisms. They harvest

energy from irregular and chaotic movements of the wrist. In contrast, myocardial contractions are continuous cyclic motions. We recently demonstrated the feasibility of harvesting heart motions using an unmodified automatic clockwork [25]. The clockwork was unmodified and therefore not adapted to work in conjunction with heart motions. For a safe and uninterrupted treatment, a reliable energy source is of key importance for pacemakers. Therefore, the energy harvesting mechanism needs to be well-adapted to generate a robust output energy from different heart contractions and orientations on the heart. The current investigation presents how the clockworks sensitivity to heart motions can be increased by optimising its oscillation weight. Our approach is divided in four parts: First, data of different heart motions were acquired and used as input for a mathematical model of the clockwork mechanism. This allows identifying essential design parameters for an optimal energy output. Second, a new prototype was developed according to these findings. Finally, in-vitro and in-vivo experiments were performed to compare the original with the new optimised oscillation weight design.

II. METHODS

A. Harvesting Principle

The presented energy harvesting device is based on an automatic clockwork. It is self-winding and autonomously recharges the battery of a wristwatch during daily use. Its energy harvesting mechanism (Fig. 1) transforms the mechanical energy of a person's wrist into electrical energy. The wrist motion is converted into rotation by means of an eccentric oscillating weight (a). A mechanical rectifier (b) transforms the oscillatory movement into a unidirectional rotation. This rotation winds a spring (c) that temporarily stores the energy in mechanical form. In this process, the spring exerts an increasing torque onto an electromagnetic generator (d). When the torque reaches the detent torque of the generator, the spring unwinds and drives the generator [29]. This leads to an electrical impulse with duration of approximately 100 ms. The spring is now completely uncoiled and the process is repeated. For generating one electrical impulse the oscillation weight needs to be deflected about 2.5 rad. With the original clockwork configuration, the induced alternating current yields an impulse with an average energy of $66.0 \pm 10.7 \mu\text{J}$. An optimal load resistance of 1000Ω has been determined by measuring the impulse energy for different load resistances connected to the generator output in a range from 80Ω to $20 \text{ k}\Omega$. This average impulse energy was considered constant because it depends on parameters such as spring stiffness, transmission gear ratio or load resistance, which remained unchanged for all experiments (in-silico, in-vitro or in-vivo, described in the following sections). The interval between two consecutive generator impulses is irregular and highly depends on the ability of the harvesting mechanism to transform the externally applied acceleration into rotation. The performance of the energy harvesting mechanism during the experiments is measured by the number of impulses for a given measurement time and is later referred to as the impulse rate f_i [s^{-1}] as common comparative value. The total mean output power

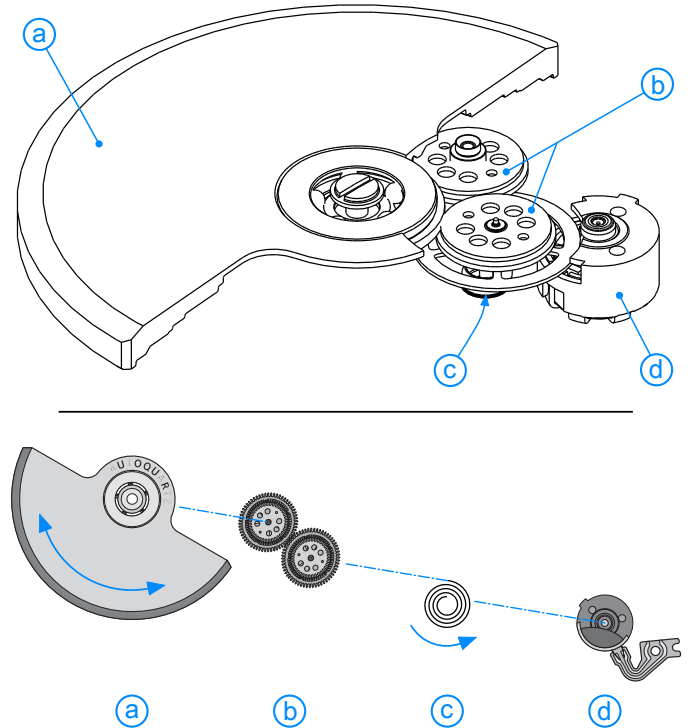


Fig. 1. The top panel represents the harvesting principle in a three-dimensional view whereas the bottom panel illustrates the energy conversion process schematically: (a) oscillation weight, (b) mechanical rectifier, (c) spring and (d) electromagnetic micro generator (courtesy of ETA SA, Switzerland).

is obtained by multiplying the energy of a single generator impulse with the impulse rate.

B. Computational Optimisation

Automatic clockworks have proved to be reliable energy sources for the watch industry. They can harvest energy from a broad spectrum of motions. However, harvesting the energy from a highly repetitive and cyclic heart motion in a reliable and efficient manner requires to adapt the system to this environment. To find the system parameters which have a strong impact on the sensitivity to heart motions, this optimisation study makes use of a mathematical model reported in [25]. The model describes the system as a two-dimensional pendulum in three-dimensional space. According to Newton's second law the pendulum's angular deflection α can be determined by the sum of all moments,

$$J\ddot{\alpha} = mr^2\ddot{\alpha} = \sum M \quad (1)$$

where m and r represent the mass and the radius to the centre of gravity of the oscillation weight, respectively. The model considers a simplified moment of inertia J for a half cylindrical disk using the material density constant for a sintered copper alloy of $\rho = 18.0 \text{ g} \cdot \text{cm}^3$. Furthermore, it accounts for different moments acting on the pendulum,

$$\ddot{\alpha} = (M_g + M_f + M_s + M_{cf} + M_{cor} + M_{eul} + M_i)/(mr^2) \quad (2)$$

which includes real moments such as gravity (M_g), friction (M_f) and the moment induced by the spring (M_s). The system was formulated in an accelerated reference frame which requires to introduce fictitious forces acting on masses in a non-inertial frame. Therefore, the model also accounts for the moments induced by the centrifugal force (M_{cf}), the Coriolis force (M_{cor}), the Euler force (M_{eul}) and the inertial force (M_i). The latter represents the reaction force to the externally applied acceleration given by the heart motion profile and acting as input of the model.

The model accounts for highly non-linear behaviours of the clockwork mechanism, for instance the spring moment that drops to 0 Nm after the sudden uncoiling of the spring. Another non-linear effect has been identified in the mechanical rectifier which translates oscillations into uni-directional rotations. This mechanism introduces a play angle of ± 15 degrees in which an oscillation of the pendulum is not actively contributing to the overall energy output. This effect has been implemented and it further improved the model's accuracy [30].

The explicit second order ordinary differential equation (2) was converted into a system of first order equations and numerically solved by using a classical 4th order Runge-Kutta algorithm with adaptive step size control. Considering the necessary angular deflection of the oscillation weight to fully charge the spring and trigger an energy impulse (2.5 rad), the cumulative angular deflection $\alpha_{cum} = \int abs(\dot{\alpha}) dt$ can be used to calculate the number of generated impulses. This allows to determine the mean output power for given average impulse energy and total simulation time.

To account for some variability among patients and implantation sites, the optimisation study uses different heart wall motion data as input for the mathematical model. These data were derived from two animal trials (AT-1 and AT-2, cf. section II-E for details). To obtain the motion data, a custom-made sensor probe has been developed utilising a 9-axis inertial measurement unit (MPU-9150, InvenSense Inc., U.S.A.). It acquired acceleration and orientation data from 6 and 7 different epicardial sites of the first and second in-vivo experiment (Fig. 2), respectively.

A parametric sweep simulation was conducted with each of the thirteen different motion profiles to optimise the oscillation weight's response to external accelerations over a broad range of motions. The sweep parameters are the radius to the centre of mass ($r \in \{2.1, 2.6, \dots, 10.6\}$ [mm]) and the mass ($m \in \{1.0, 1.5, \dots, 9.5\}$ [g]) of the oscillation weight.

C. Prototyping

Three prototypes were constructed for the in-vitro and in-vivo experiments (section II-D and II-E) which we later refer to as mass imbalance oscillation generator (MIOG 1, 2 and 3, cf. Fig. 3). All of them are based on the automatic clockwork ETA 204 (ETA SA, Switzerland), comprising an electromagnetic micro generator MG205 (Kinetron B.V., the Netherlands). They are protected by a custom made housing providing six eyelets for suturing the device onto the heart. The housing was 3D printed (Alaris30, Objet Ltd., Israel)

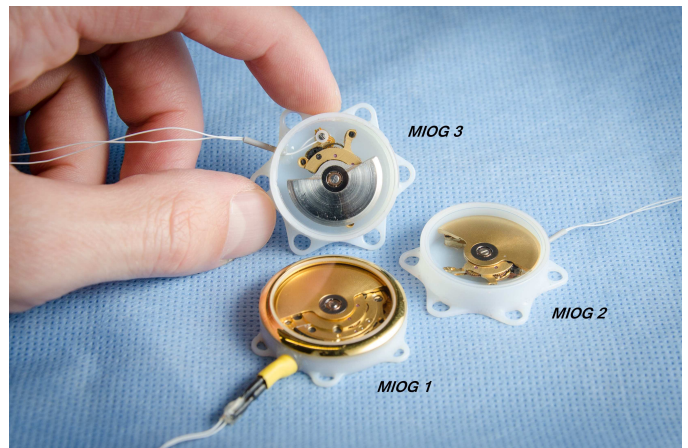


Fig. 3. The three harvesting devices: MIOG 1 featuring the original oscillation weight, the original clockwork and the glass lid; MIOG 2 featuring the old oscillation weight, the skeletonized clockwork and the polycarbonate lid; MIOG 3 featuring the optimised oscillation weight, the skeletonized clockwork and the polycarbonate lid.

out of polymer VeroWhite FullCure830 (Objet Ltd.). The devices differ from each other by three features: the oscillation weight, the clockwork's mass and the housing lid (cf. Table I). All clockworks were stripped from unnecessary time-indicating parts to keep the bare energy harvesting mechanism. Whereas MIOG 1 (original clockwork described in [25]) remained unmodified, the clockworks of MIOG 2 and 3 were skeletonized to further lower the device weight and therefore ease the burden on the heart. For the same reason the original glass lid with the metallic frame in MIOG 1 was replaced by a lighter polycarbonate lid in MIOG 2 and 3.

Due to their similar setup, MIOG 2 and 3 qualify for comparing the performance of the different oscillation weights and are therefore the focus of this study. MIOG 1 and 2 were used in the in-vivo experiment to observe the influence of the different device weights.

D. In-vitro validation

For the in-vitro validation of the MIOGs, a Stewart platform has been developed to mimic complex three-dimensional heart motions. The structure of this parallel robot allows moving the platform in all 6 degrees of freedom (3D translations and 3D rotations). All the previously recorded heart wall motions of AT-1 and AT-2 (cf. section II-B) served as input for the Stewart platform. Its end-effector features a gimbal-lock mechanism to fixate the MIOG and align its initial orientation in the field of gravity. This allows positioning the devices on the Stewart platform in the same orientation as measured by the sensor probe at each of the thirteen locations on the heart. The robot was programmed to replicate a heart motion profile over a period of five minutes. These cycles were repeated three times for each position and MIOG to measure the resulting impulse rate.

The Stewart platform moves the devices along a given trajectory. Since MIOG 1 and 2 are identical except for their overall mass, only MIOG 2 and 3 were used in this in-vitro experiment.

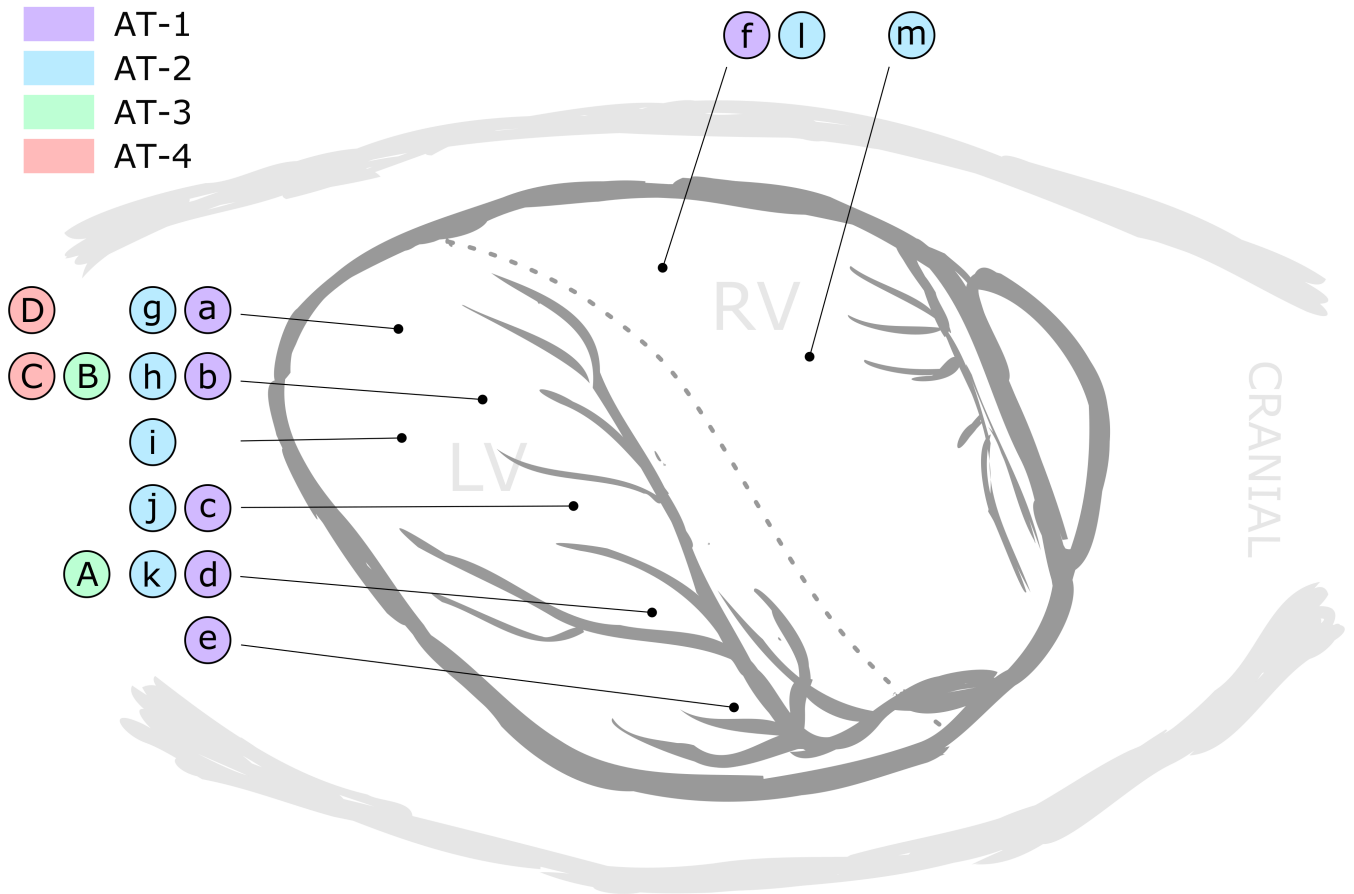


Fig. 2. The labels indicate the approximate location of all thirteen points on the heart measured by the acceleration sensor during AT-1 (purple, a-f) and AT-2 (blue, g-m) and the four positions where the MIOGs have been tested during AT-3 (green, A and B) and AT-4 (red, D and C). The acceleration measurements were performed on a diagonal pathway from an antero-apical site (a and g) to a mid-lateral site of the left ventricle. In three additional acceleration measurements, data from the mid-lateral (f and l) and antero-basal site (m) on the right ventricle were acquired.

TABLE I
 PROPERTIES OF THE DIFFERENT MIOG DEVICES.

	MIOG 1	MIOG 2	MIOG 3
total weight	16.7 g	7.2 g	11.4 g
oscillation weight	original (3.6 g)	original (3.6 g)	optimised (7.7 g)
mass clockwork	7.6 g	1.3 g (skeletonized)	1.3 g (skeletonized)
lid design	original glass lid (4.8 g)	polycarbonate lid (0.7 g)	polycarbonate lid (0.7 g)

E. In-vivo validation

In total, four animal trials (AT-1 to -4) were successively performed on 60 kg domestic pigs. The pigs were under inhalation anaesthesia and placed in recumbent position. The trials were approved by the Swiss Federal Veterinary Office and performed in compliance with the Guide for the Care and Use of Laboratory Animals [31]. Thoracotomy and pericardiectomy allowed the fixation of the devices onto the heart.

During AT-1 and AT-2 the inertial measurement sensor measured thirteen heart motion profiles which later served as input for the mathematical model.

After the in-silico optimisation, all MIOGs were validated during the in-vivo studies AT-3 and AT-4. The devices were tested at two different locations on the left ventricle (Fig. 2,

AT-3: position A and B, AT-4: position C and D). To facilitate the attaching and detaching of the MIOGs on the epicardium, an adapter ring was introduced. The ring was 3D printed (Alaris30, Material: VeroWhite FullCure830) and features a bayonet mount that holds the device in position. Once sutured to the epicardium, the ring allows an easy exchange of the prototypes and guarantees that all devices were tested at the same location on the heart. In addition, the orientation with respect to the gravity field was adjusted by tilting the operating table about ± 20 degrees along the cranio-caudal axis of the pig. Each of the three devices was tested on two hearts (AT-3 and AT-4), at two locations on the heart (position A-D, cf. Fig. 2) and at three orientations (-20 , 0 and $+20$ degree OR table tilting angle). This amounts to 36 individual experiments each lasting 60 seconds. During a cumulative testing period

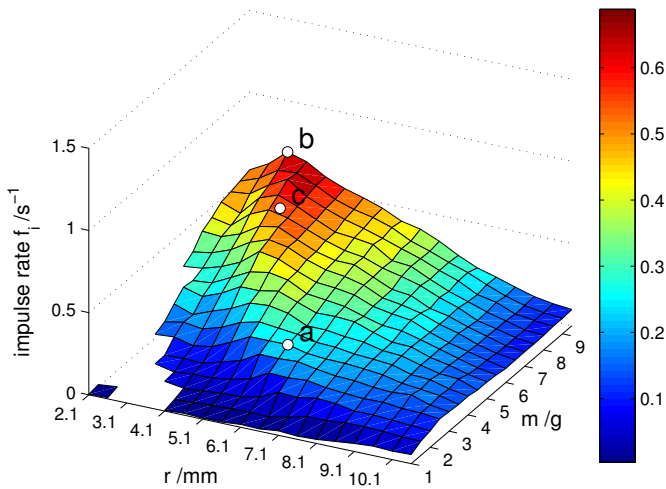


Fig. 5. Averaged impulse rate over all thirteen motion profiles, showing the theoretical potential for improvement (b: $r = 3.1$ mm, $m = 9.5$ g and $f_i \approx 0.69$ s⁻¹) with respect to the original oscillation weight configuration (a: $r = 6.1$ mm, $m = 3.5$ g and $f_i \approx 0.26$ s⁻¹). Point c depicts the impulse rate for the final implementation (MIOG 3) with $r = 3.8$ mm, $m = 7.7$ g and $f_i \approx 0.56$ s⁻¹.

of 36 minutes, a variation of the heart rate is likely and might affect the performance of a MIOG. To compensate for this natural variation the measured impulse rates were normalised to a heart rate of 90 bpm.

For testing a device at three different OR table tilting angles it stayed approximately 10 minutes on the heart. Therefore, each device was mounted on the heart over a period of about 40 minutes in total (on two positions in each of the two animal trials). All experiments were performed in an open-chest scenario.

III. RESULTS

A. Computational Optimisation

The optimisation study was conducted for all thirteen different motion profiles. The parametric sweep result for each motion profile shows an increased energy output for oscillation weights with a smaller radius and a higher mass (Fig. 4). Furthermore, the model predicts high impulse rates reaching up to $f_i \approx 1.43$ s⁻¹ for motion profiles at antero-apical (a-c and g-i) and right ventricular regions (f, l and m) whereas an impulse rate of only about $f_i \approx 0.35$ s⁻¹ is predicted at mid-lateral positions (d-e and j-k).

The averaged output of the parametric sweep simulations (Fig. 5) shows a tendency for a common optimal radius and mass of the oscillation weight at 3.1 mm and 9.5 g, respectively. For this configuration, the mathematical model predicts an averaged impulse rate of 0.69 ± 0.47 s⁻¹ and shows a theoretical superiority towards the original configuration ($r = 6.1$ mm and $m = 3.5$ g) of about 270 % (0.26 s⁻¹).

B. Prototyping

The computational optimisation yielded the design parameters that maximize the theoretical output energy. However, in a real implantation, these parameters may have to be adjusted

due to physical restrictions (e.g., related to manufacturing). In MIOG 3, an optimized oscillation weight with a radius of 3.8 mm and a mass of 7.7 g was used. For this configuration, the in-silico model predicts an impulse rate of about $f_i \approx 0.56 \pm 0.37$ s⁻¹ (Fig. 5, point c). It is made of a platinum alloy (Pt 950, material density ≈ 20.2 g · cm⁻³) by 3D metal printing (Altmann-Casting, Switzerland) and finished in a conventional milling process. The skeletonizing process reduced the mass of the clockworks of MIOG 2 and 3 by 80 % from the original 7.6 g to 1.3 g.

C. In-vitro

The Stewart platform successfully accelerated MIOG 2 and 3 using all thirteen motion profiles. Figure 6 illustrates the results of the in-vitro experiment where a single bar represents a 5-minute experiment. For all experiments, the MIOGs achieved a highly reproducible impulse rate. The measured impulse rates for MIOG 2 (blue) and MIOG 3 (red) follow the trend predicted by the computational model (triangular markers): accelerations from antero-apical (a-c and g-i) and right ventricular sites (f, l and m) lead to higher impulse rates compared to accelerations from mid-lateral locations (d-e and j-k). By comparing the results from MIOG 2 and 3, the superiority of the new optimized oscillation weight (MIOG 3) can be observed regardless of the motion profiles (i. e. the implantation site). Furthermore, MIOG 3 generated enough energy to power a modern cardiac pacemaker (black dashed line, 6 μW according to the reference manual of Nanostim TM, St. Jude Medical) at all tested motion scenarios.

D. In-vivo

An average heart rate of 86 ± 9 bpm and 88 ± 5 bpm was measured during AT-3 and AT-4, respectively. In both trials, fixation of the devices onto the heart did not influence the vital parameters. Regardless of the operating table tilting angle the optimised MIOG 3 is superior to both other prototypes (Fig. 7 (a), each bar represents the average result for the three operating table tilting angle). MIOG 3 exceeded the required impulse rate for powering a cardiac pacemaker (black dashed line) in both animal trials at one position. As illustrated in Figure 7 (b), the impulse rate is influenced by tilting the pigs body and therefore changing the devices orientation in space when averaging the results for both trials and positions. Also in this perspective MIOG 3 is superior to both other devices.

IV. DISCUSSION

The presented energy harvesting concept proved able to convert heart motions into electrical energy. A dedicated mathematical model was successfully employed to improve the oscillation weights sensitivity to heart motions. By testing different heart motion profiles, this work demonstrates that the energy output is strongly affected by the devices location and orientation on the heart and that the clockwork mechanism requires an adequate optimisation. In-vitro and in-vivo results have shown a significantly improved impulse rate for the new optimised oscillation weight.

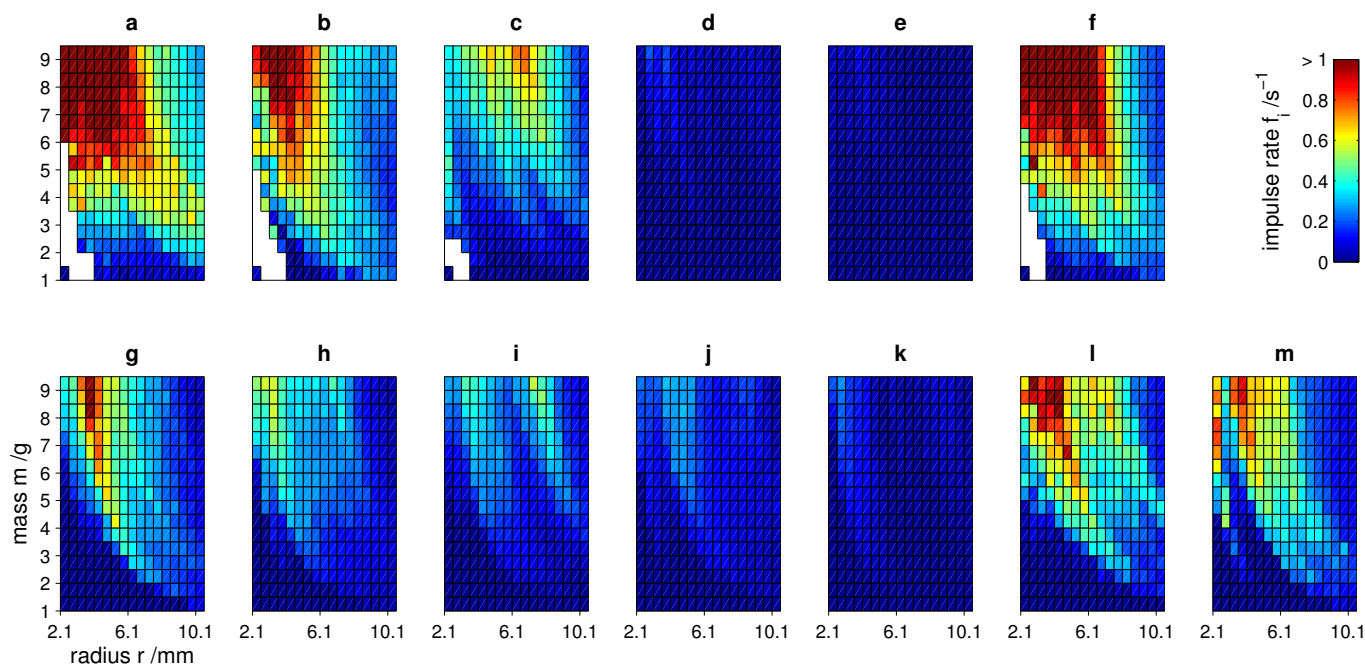


Fig. 4. Results of the parametric sweep optimisation for all thirteen different motion profiles recorded during animal trial AT-1 (top row: a-f) and AT-2 (bottom row: g-m). Dark red coloured areas indicate high impulse rates.

This study illustrates an important factor for designing devices that harvest kinetic energy from the heart by an oscillation weight: Affixing the device to a location on the myocardium where it experiences strong accelerations in its plane of motion is crucial for its performance. In addition, the devices orientation in space changes the effect of gravity on the device. Especially in a vertical orientation when the oscillation mass points in direction of gravity and the internal spring is nearly charged, a strong excitation is needed to overcome the threshold torque for generating an impulse. This issue is even more pronounced due to the rectifying mechanism, which is translating the oscillatory rotation into a unidirectional rotation and thereby introduces a dead angle of 30 degrees [30]. To prevent such a scenario, the rectifying mechanism could be replaced by a ratchet mechanism to achieve a torque-free rotation in one direction so that the oscillation weight can liberate itself from a deadlock. Future investigation will show how this modification affects the harvesters output energy.

The oscillation weight is the mechanisms key component. Changing its design will inevitably affect its sensitivity to external excitations. For heart motions we have shown that a smaller radius and a higher mass increase the systems sensitivity and ultimately the output energy. To reduce the computational effort as well as the prototyping complexity, the optimisation was limited to two sweep parameters (radius and mass) whereas other parameters such as the spring constant, transmission gear ratio or load resistance were not changed. Even though these parameters have no direct influence on the oscillation weights sensitivity they can affect the resisting torque and therefore influence the harvesters impulse rate. A decreasing spring constant, for instance, would reduce the generators impulse energy, lower the torque for the oscillation

weight and thereby increase the impulse rate. Furthermore, this might also yield another global optimum for the weights radius and mass. These considerations are part of ongoing investigations. However, they will increase the complexity of the optimisation process and lead to major alterations in the design of the conversion mechanism.

The presented harvesting devices have proven the feasibility of harvesting low frequency vibrations of a heart. However, the natural resonance frequency of the tested oscillation weights is at about 4 Hz and therefore will not match the fundamental frequency of a heart rate between 40 and 200 beats per minute ($\approx 0.6 - 3.3$ Hz). Nevertheless, in rare occasions a prototype can resonate at a harmonic frequency of the present heart motion. This might also explain the unusually good performance of MIOG 2 during animal trial AT-3 at position B.

Furthermore, it seems surprising that MIOG 1 outperforms the much lighter MIOG 2 in three out of four in-vivo experiments. However, measurements have shown that when the heart is loaded with an additional mass, it contracts more powerfully to maintain an adequate cardiac output [32]. This increases the harvester's output power, but it contradicts the basic principle that energy harvesting should not require the host to perform extra work.

The results of the in-silico and in-vitro experiments illustrate a clear tendency (Fig. 4). Even though both experiments base on the same heart motion profiles as input, some of them (e.g. b, f, g and m) show a large discrepancy in impulse rate. This error arises from the fact that the tested profiles comprise motion patterns with high accelerations and are difficult to accurately mimic by the Stewart Platform. Due to the rather chaotic behaviour of the energy harvester, small changes in the motion trajectory can either positively or negatively affect

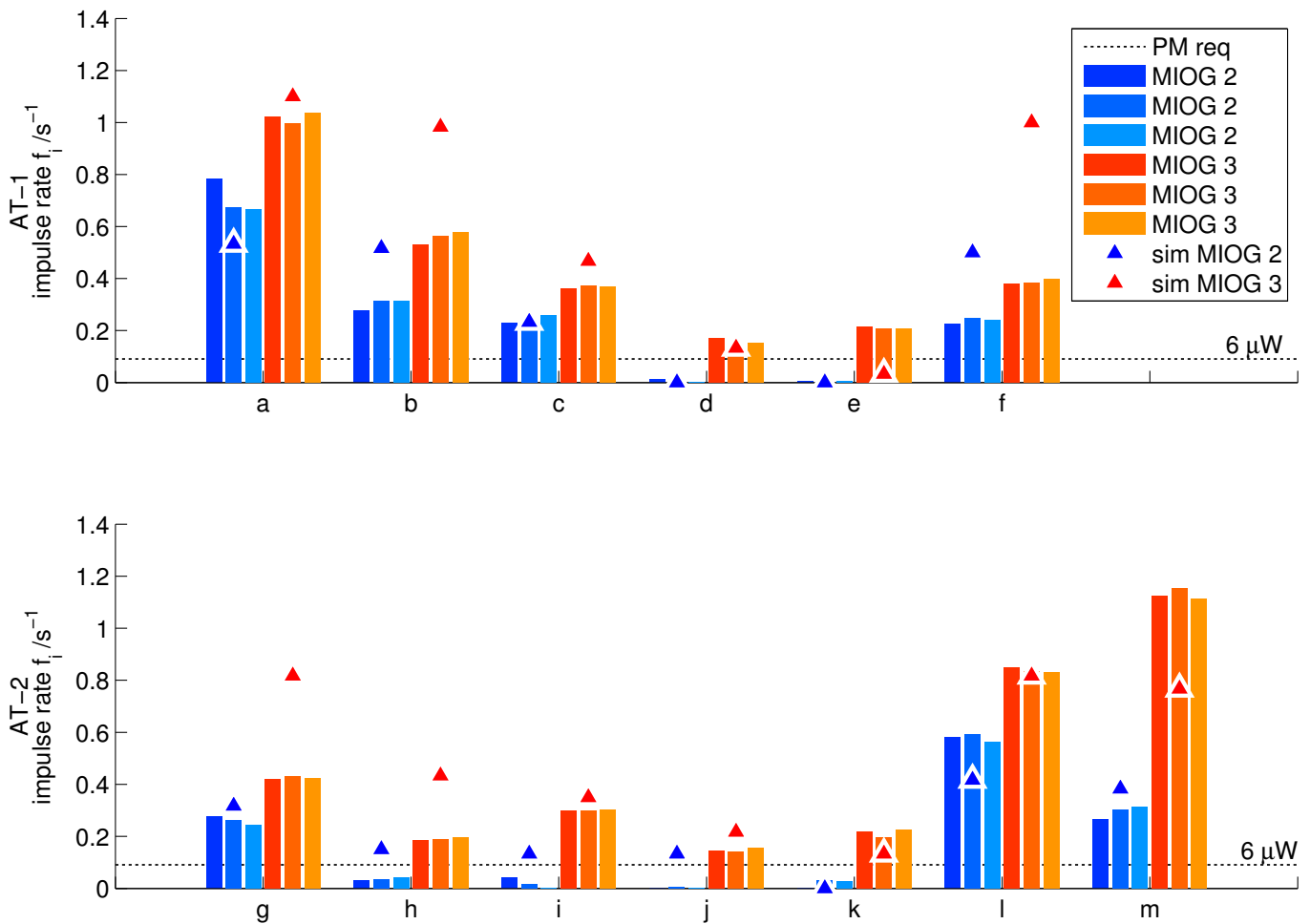


Fig. 6. The impulse rates at which MIOG 2 (blue) and MIOG 3 (red, optimised oscillation weight) harvested the energy during the in-vitro experiment. The different colour grading for blue and red show the results for three identical experiments. The Stewart platform accelerated the devices according to all thirteen motion profiles which were recorded during animal trials AT-1 (top row: a-f) and AT-2 (bottom row: g-m). In addition, the blue and red triangular markers represent the impulse rate predicted by the mathematical model (sim MIOG). The black dotted line indicates the minimum required impulse rate to power a cardiac pacemaker (PM).

the impulse rate.

As a power supply for cardiac pacemakers, the harvesting device is supposed to remain on the ventricle for a long period of time. Therefore, chronic in-vivo trials will be required, first, to show the reaction of the heart to the additional load and second, to investigate how the harvester efficiency is affected by potential changes of heart contractions. It is expected that the heart copes with the new situation by increasing the myocardial volume to compensate for the additional load. Since the presented harvesting mechanism can harvest from many different heart contractions, the new tissue formation might even introduce a advantageous effect on the energy extraction rate.

The reliability of a pacemaker is of key importance to provide a continuous treatment and guarantee the safety of a patient. Therefore, the pacemaker electronics would need to temporarily store the generated energy in a buffer energy storage to overcome periods of energy shortage (e.g. heart or system failures). Capacitors and secondary batteries are commonly used for this purpose but suffer from large leakage currents and limited number of recharging cycles, respectively.

However, advances in solid-state battery technology indicate a potential solution to avoid both limitations [33]. Due to their small packaging and safe composition (no liquid electrolyte), solid-state batteries may become an ideal complement for energy harvesting devices in the future.

To estimate the harvester's conversion efficiency the mean power invested by the heart to accelerate the device on the ventricle needs to be approximated. As demonstrated in an in-vivo case study [32], the heart spent a mean power of $220 \mu W$ for accelerating an additional load of $12.5 g$ attached to the antero-apical site of a left ventricle. Considering a mean impulse energy of $66 \mu J$ and a mean impulse rate of $f_i = 0.56 s^{-1}$ for MIOG 3 ($11.4 g$) the conversion efficiency for this specific case is 16.8% . The conversion efficiency depends on the heart motion profile and is likely to change for different implantation sites or inter-species differences.

At the current development state of the prototype, the housing has a very functional purpose to facilitate in-vitro and in-vivo investigations. Its transparent lid allows a good visual control of the prototype performance but presents rough edges toward the pericardium. Therefore, an epicardial implantation

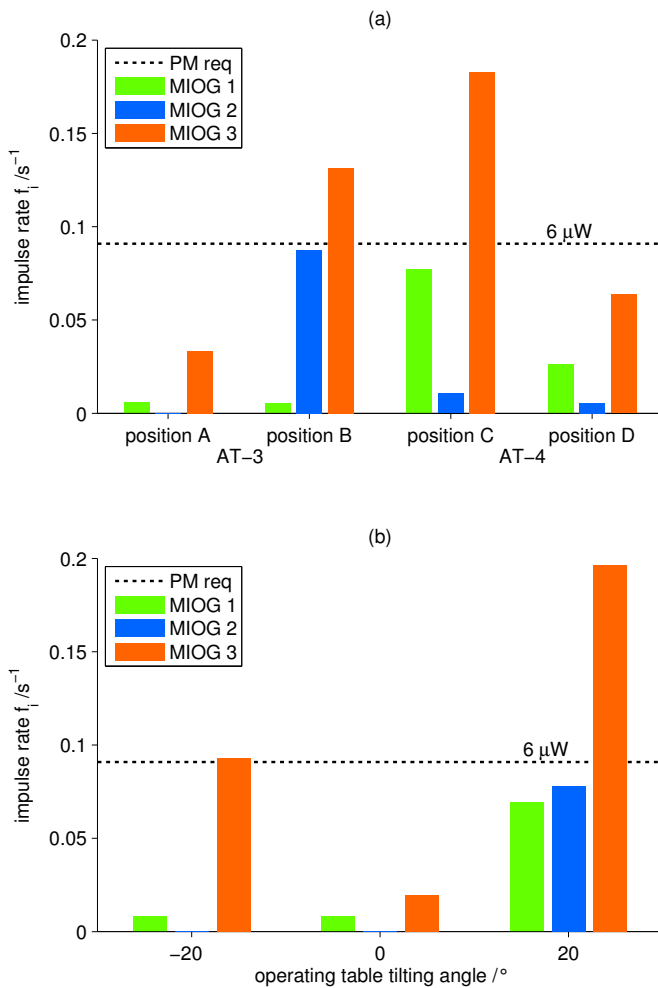


Fig. 7. a) Illustrates the in-vivo results of all tested MIOGs (MIOG 1 (green), MIOG 2 (blue) and MIOG 3 (red)) with respect to different positions on the heart (Fig. 2, position A-D). Each bar represents the averaged results of the three operating table tilting angle. b) Depicts the influence of the operating table tilting angle on all tested MIOGs. Each bar represents the averaged results of the four tested positions A-D. The black dotted line indicates the minimum impulse rate required to power a cardiac pacemaker (PM).

site would call for an appropriate device packaging to ensure a rigid fixation on the epicardium and to present a smooth surface towards the pericardium. In addition, the hermicity of the device could be improved by using an appropriate material (e.g. titanium alloys) or by a parylene - silicon oxide multilayer thin-film coating [34], [35]. Furthermore, the device is not yet optimised to be used in conjunction with cardiac motions and would require a new design with an optimised shape and size.

V. CONCLUSION

In this study we successfully increased the sensitivity of an automatic clockworks oscillation weight to heart motions by means of a dedicated mathematical model. Testing our energy harvesting device with different heart motions revealed a strong relation between the harvested amount of energy and the position and orientation of the device on the heart.

ACKNOWLEDGMENT

We thank Stijn Vandenberghe for his support and valuable advice. Our gratitude extends to the entire team of the Experimental Surgery Institute of the Inselspital Bern for their support in animal studies. Furthermore, we thank Otto Aeby and Danael Gasser of the Department of Clinical Research and the ARTORG Center (University of Bern, Switzerland) for their assistance in mechanical manufacturing. The research was supported by the Commission for Technology and Innovation (KTI-CTI 12589.1 PFLS-LS), the Research Funds of the Department of Cardiology at the Bürgerspital Solothurn, Switzerland and the Department of Cardiology at the Bern University Hospital, Switzerland.

REFERENCES

- [1] L. Mateu and F. Moll, "Review of energy harvesting techniques and applications for microelectronics," in *SPIE 5837, VLSI Circuits and Systems II*, vol. 5837. SPIE, Jun. 2005, pp. 359–373.
- [2] J. Paradiso and T. Starner, "Energy Scavenging for Mobile and Wireless Electronics," *IEEE Pervasive Computing*, vol. 4, no. 1, pp. 18–27, Jan. 2005.
- [3] T. Starner, "Human-powered wearable computing," *IBM Systems Journal*, vol. 35, no. 3.4, pp. 618–629, 1996.
- [4] E. Romero, R. O. Warrington, and M. R. Neuman, "Energy scavenging sources for biomedical sensors," *Physiological measurement*, vol. 30, no. 9, pp. R35–62, 2009.
- [5] S. R. Platt, S. Farritor, K. Garvin, and H. Haider, "The use of piezoelectric ceramics for electric power generation within orthopedic implants," *IEEE/ASME Transactions on Mechatronics*, vol. 10, no. 4, pp. 455–461, Aug. 2005.
- [6] P. Niu, P. Chapman, R. Riemer, and X. Zhang, "Evaluation of motions and actuation methods for biomechanical energy harvesting," in *Power Electronics Specialists Conference, 2004. PESC 04. 2004 IEEE 35th Annual*, vol. 3, Jun. 2004, pp. 2100–2106 Vol.3.
- [7] N. Lajnef, N. Elvin, and S. Chakrabarty, "A Piezo-Powered Floating-Gate Sensor Array for Long-Term Fatigue Monitoring in Biomechanical Implants," *IEEE Transactions on Biomedical Circuits and Systems*, vol. 2, no. 3, pp. 164–172, Sep. 2008.
- [8] S. Kerzenmacher, J. Ducre, R. Zengerle, and F. von Stetten, "Energy harvesting by implantable abiotically catalyzed glucose fuel cells," *Journal of Power Sources*, vol. 182, no. 1, pp. 1–17, Jul. 2008.
- [9] A. Haeberlin, A. Zurbuchen, J. Schaerer, J. Wagner, S. Walpen, C. Huber, H. Haeberlin, J. Fuhrer, and R. Vogel, "Successful pacing using a batteryless sunlight-powered pacemaker," *Europace*, vol. 16, no. 10, pp. 1534–1539, Oct. 2014.
- [10] A. Haeberlin, A. Zurbuchen, S. Walpen, J. Schaerer, T. Niederhauser, C. Huber, H. Tanner, H. Servatius, J. Seiler, H. Haeberlin, J. Fuhrer, and R. Vogel, "The first batteryless, solar-powered cardiac pacemaker," *Heart Rhythm*, Mar. 2015.
- [11] S. Ayazian, V. Akhavan, E. Soenen, and A. Hassibi, "A Photovoltaic-Driven and Energy-Autonomous CMOS Implantable Sensor," *IEEE Transactions on Biomedical Circuits and Systems*, vol. 6, no. 4, pp. 336–343, Aug. 2012.
- [12] Y. Qin, X. Wang, and Z. L. Wang, "Microfibre-nanowire hybrid structure for energy scavenging," *Nature*, vol. 451, no. 7180, pp. 809–813, Feb. 2008.
- [13] Z. Wang, V. Leonov, P. Fiorini, and C. Van Hoof, "Realization of a wearable miniaturized thermoelectric generator for human body applications," *Sensors and Actuators A: Physical*, vol. 156, no. 1, pp. 95–102, Nov. 2009.
- [14] F. Staehle, B. A. Jung, S. Bauer, J. Leupold, J. Bock, R. Lorenz, D. Fil, and M. Markl, "Three-directional acceleration phase mapping of myocardial function," *Magnetic Resonance in Medicine*, vol. 65, no. 5, pp. 1335–1345, 2011.
- [15] A. Pfenniger, M. Jonsson, A. Zurbuchen, V. M. Koch, and R. Vogel, "Energy Harvesting from the Cardiovascular System, or How to Get a Little Help from Yourself," *Annals of Biomedical Engineering*, vol. 41, no. 11, pp. 2248–2263, Nov. 2013.
- [16] A. Pfenniger, R. Vogel, V. M. Koch, and M. Jonsson, "Performance analysis of a miniature turbine generator for intracorporeal energy harvesting," *Artificial Organs*, vol. 38, no. 5, pp. E68–81, May 2014.

- [17] M. Jonsson, A. Zurbuchen, A. Haeblerlin, A. Pfenniger, and R. Vogel, "Vascular turbine powering a cardiac pacemaker: an in-vivo case study," *Experimental and clinical cardiology*, vol. 20, no. 1, pp. 2000–2003, 2014.
- [18] M. Deterre, E. Lefeuvre, Y. Zhu, M. Woytasik, B. Boutaud, and R. Dal Molin, "Micro Blood Pressure Energy Harvester for Intracardiac Pacemaker," *Journal of Microelectromechanical Systems*, vol. 23, no. 3, pp. 651–660, Jun. 2014.
- [19] P. Roberts, G. Stanley, and J. M. Morgan, "Abstract 2165: Harvesting the Energy of Cardiac Motion to Power a Pacemaker," *Circulation*, vol. 118, no. 18 Supplement, p. S_679, Oct. 2008.
- [20] M. A. Karami and D. J. Inman, "Powering pacemakers from heartbeat vibrations using linear and nonlinear energy harvesters," *Applied Physics Letters*, vol. 100, no. 4, pp. 042 901–042 901–4, Jan. 2012.
- [21] C. Dagdeviren, B. D. Yang, Y. Su, P. L. Tran, P. Joe, E. Anderson, J. Xia, V. Doraiswamy, B. Dehdashti, X. Feng, B. Lu, R. Poston, Z. Khalpey, R. Ghaffari, Y. Huang, M. J. Slepian, and J. A. Rogers, "Conformal piezoelectric energy harvesting and storage from motions of the heart, lung, and diaphragm," *Proceedings of the National Academy of Sciences*, p. 201317233, Jan. 2014.
- [22] H. Li, C. Tian, and Z. D. Deng, "Energy harvesting from low frequency applications using piezoelectric materials," *Applied Physics Reviews*, vol. 1, no. 4, p. 041301, Dec. 2014.
- [23] M. H. S. Alrashdan, A. A. Hamzah, and B. Majlis, "Design and optimization of cantilever based piezoelectric micro power generator for cardiac pacemaker," *Microsystem Technologies*, pp. 1–11, Oct. 2014.
- [24] H. Goto, T. Sugiura, Y. Harada, and T. Kazui, "Feasibility of using the automatic generating system for quartz watches as a leadless pacemaker power source," *Medical & Biological Engineering & Computing*, vol. 37, no. 3, pp. 377–380, 1999.
- [25] A. Zurbuchen, A. Pfenniger, A. Stahel, C. T. Stoeck, S. Vandenberghe, V. M. Koch, and R. Vogel, "Energy Harvesting from the Beating Heart by a Mass Imbalance Oscillation Generator," *Annals of Biomedical Engineering*, vol. 41, no. 1, pp. 131–141, Jan. 2013.
- [26] E. O. Udo, N. P. A. Zuithoff, N. M. van Hemel, C. C. de Cock, T. Hendriks, P. A. Doevendans, and K. G. M. Moons, "Incidence and predictors of short- and long-term complications in pacemaker therapy: The FOLLOWPACE study," *Heart Rhythm*, vol. 9, no. 5, pp. 728–735, 2012.
- [27] H. G. Mond and A. Proclemer, "The 11th World Survey of Cardiac Pacing and Implantable Cardioverter-Defibrillators: Calendar Year 2009A World Society of Arrhythmia's Project," *Pacing and Clinical Electrophysiology*, vol. 34, no. 8, pp. 1013–1027, 2011.
- [28] E. B. Fortescue, C. I. Berul, F. Cecchin, E. P. Walsh, J. K. Triedman, and M. E. Alexander, "Patient, procedural, and hardware factors associated with pacemaker lead failures in pediatrics and congenital heart disease," *Heart Rhythm*, vol. 1, no. 2, pp. 150–159, Jul. 2004.
- [29] M. Lossec, B. Multon, and H. Ben Ahmed, "Micro-kinetic generator: Modeling, energy conversion optimization and design considerations," in *MELECON 2010 - 2010 15th IEEE Mediterranean Electrotechnical Conference*, Apr. 2010, pp. 1516 –1521.
- [30] A. Zurbuchen, A. Pfenniger, S. Omari, and R. Vogel, "Modelling and Validation of a Mass Imbalance Oscillation Generator to Harvest Heart Motion Energy," in *24th International IASTED Conference on Modelling and Simulation, 2013*. ACTA Press, Jul. 2013.
- [31] National Research Council (US) Committee for the Update of the Guide for the Care and Use of Laboratory Animals, *Guide for the Care and Use of Laboratory Animals*, 8th ed., ser. The National Academies Collection: Reports funded by National Institutes of Health. Washington (DC): National Academies Press (US), 2011.
- [32] A. Zurbuchen, A. Haeblerlin, J. Schaerer, A. Pfenniger, and R. Vogel, "Harvesting energy from the heart wall motion - Device weight considerations," *Biomedical Engineering / Biomedizinische Technik*, vol. 59, no. s1, p. s227, 2014.
- [33] Y. Wang, W. D. Richards, S. P. Ong, L. J. Miara, J. C. Kim, Y. Mo, and G. Ceder, "Design principles for solid-state lithium superionic conductors," *Nature Materials*, vol. 14, no. 10, pp. 1026–1031, 2015.
- [34] A. Hogg, T. Aellen, S. Uhl, B. Graf, H. Keppner, Y. Tardy, and J. Burger, "Ultra-thin layer packaging for implantable electronic devices," *Journal of Micromechanics and Microengineering*, vol. 23, no. 7, p. 075001, 2013.
- [35] A. Hogg, S. Uhl, F. Feuvrier, Y. Girardet, B. Graf, T. Aellen, H. Keppner, Y. Tardy, and J. Burger, "Protective multilayer packaging for long-term implantable medical devices," *Surface and Coatings Technology*, vol. 255, pp. 124–129, Sep. 2014.